Zeitschrift: Comtec : Informations- und Telekommunikationstechnologie = information and telecommunication technology

Herausgeber: Swisscom

Band: 75 (1997)

Heft: 5

Artikel: Some examples of atmospheric effects on laser beam propagation

Autor: Loémbé, André

DOI: https://doi.org/10.5169/seals-876934

ATMOSPHERIC LASER-BASED TRANSMISSION SYSTEM

SOME EXAMPLES OF ATMOSPHERIC EFFECTS ON LASER BEAM PROPAGATION

As the technology of laser sources continues to advance, there is renewed interest in using optical wavelengths as carriers of information in line-of sight (LOS) communication systems. The use of such systems for short ranges, up to about 1 km, is being considered a valuable alternative or extension to digital microwave radio systems, since they can be operational in a very short period of time.

ANDRÉ LOÉMBÉ, BERN

Typical areas where these systems could be applied include:

- interconnections of two local area networks (LANs) located in different office buildings
- links for bridging streets, highways, rivers, or train rails
- links between base stations in mobile telephone systems
- easy and quick installation of TV transmissions for temporary events

One of the advantages of such transmission systems is that they require less transmitting power due to their extremely narrow beam, which can contribute to communication security. An atmospheric laser-based system does not create interference, neither with conventional microwave systems nor with other laser systems. A further advantage is that, whenever an easy and quick installation for short-distance communications is needed, it provides a good alternative for significant cost savings.

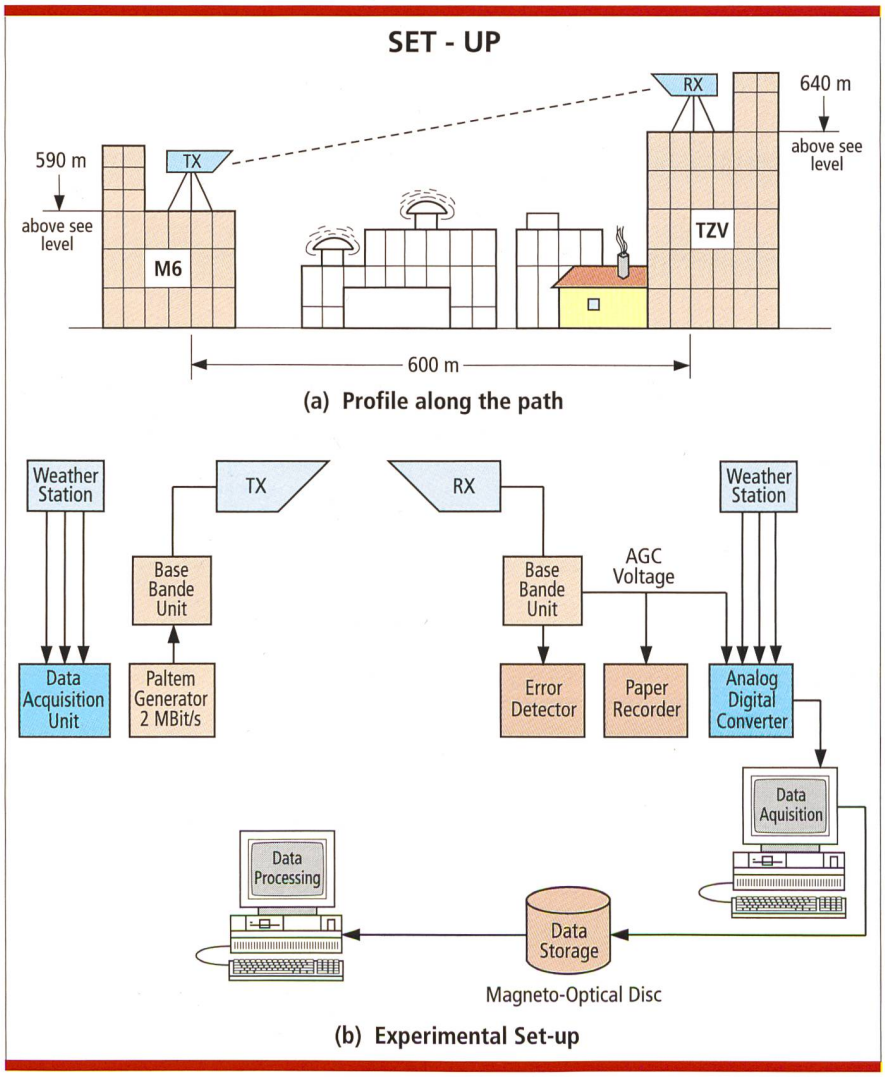

Fig. 1. a) Profile along the path. b) Experimental set-up.

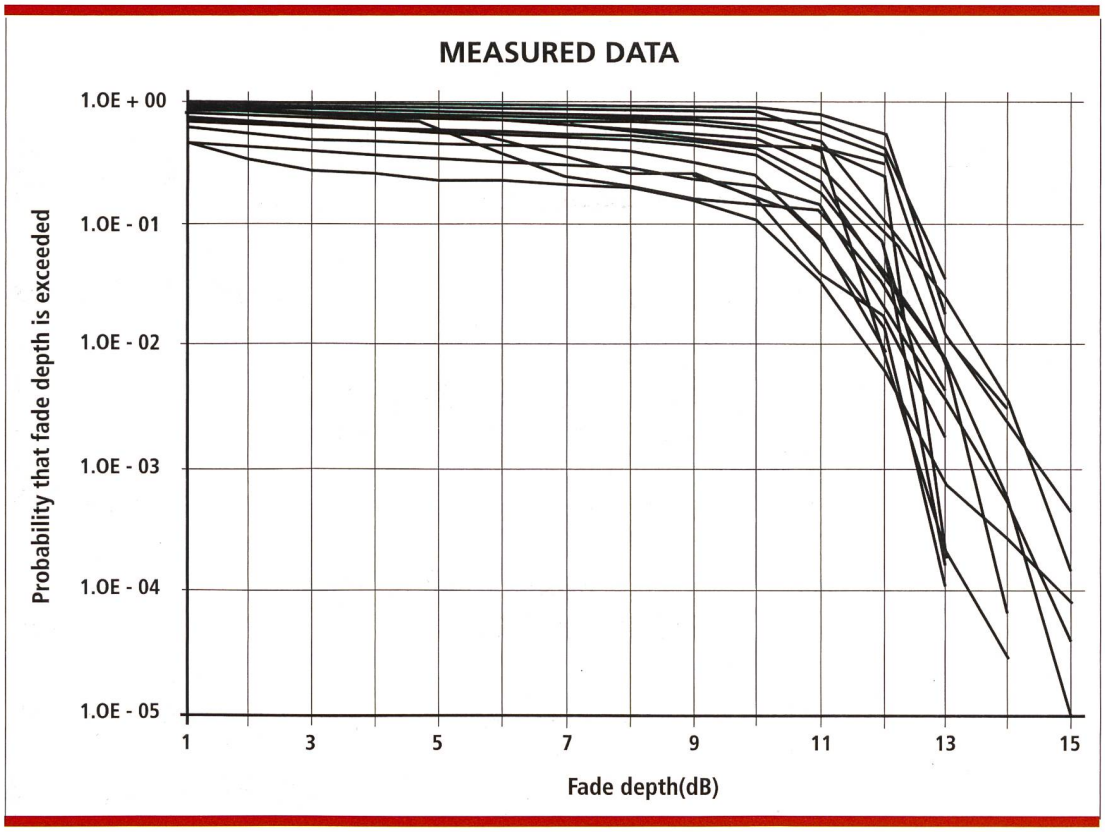

Fig. 2. Monthly probability of exceeding a given fade depth. Measured data from 1 February 1993 to 31 May 1994.

Objectives of the experiment

When propagating through suspended small particles (aerosols, or through turbulence in the earth's atmosphere, laser beams may experience intensity reduction, and the wave front of the beam may become distorted, giving rise to bit errors; however, the extent to which such wavefront distortions affect the error performance and the quality of the information signal is unknown.
The current experiment aims at evaluating the performance of such a system in terms of reliability, quality, and availability under real propagation conditions. In addition, it quantifies the effects of the atmospheric channel on the propagation of 0.78-μm laser beam as carrier of information signal as well.

Experimental setup

Figure 1 shows the various components of the experimental setup and the path profile. The installation platforms ensure very good mechanical stability to the transmitter and the receiver. The predominant environment along the path is an industrial zone (Figure 1a), and the link extends over a 600-m path length, but, according to the manufacturer, this can be as long as 1 km. The experiment was carried out with a commercial equipment which utilizes a 20 mW continuous wave laser diode as near-infrared optical source at wavelength $\lambda = 0.78$ μm (f = 385 THz). This wavelength is located within a so-called 'atmospheric transmission window' (i.e. 0.4 to 0.8 μm), which is one of the low-absorption bands of the spectrum [1].

Atmospheric laser-based transmission system

The transmission equipment consists of a transmitter, an optical receiver, and a removable telescopic sight for easy link alignment. The transmitter, in conjunction with a collimating lens, utilizes a solid-state GaAlAs-laser diode to produce a narrow beam of light which carries the data signal. The receiver, in conjunction with a collecting lens and an optical bandpass filter, utilizes a low-noise PIN photodiode to detect and recover the originally transmitted data signal from the incoming beam. The standard and optional interfaces of the equipment include: video (6 MHz bandwidth), data (RS232), PCM (G.703), audio (baseband), and IEEE 802.3 (Ethernet).
Although the system under consideration can operate in duplex mode, the experiment was conducted in simplex mode (unidirectional transmission) at a transmission rate of 2.048 Mbit/s.

Weather stations

To reach the above-mentioned objectives, weather stations have been installed near the receiver and the transmitter as indicated in Figure 1b. A heated tipping bucket rain gauge (resolution: 0.1 mm/tip; integration time: 1 min) has also been installed at about 10 m from the receiver. Meteorological data on air temperature, relative humidity, and barometric pressure are simultaneously measured and recorded. These data are used to investigate the correlation between atmospheric conditions and received signal degradation.

Data acquisition system

The data acquisition equipment is shown in Figure 1b. Two kinds of signals are interfaced to the computer: the analog signals (AGC, air tempera-

P_{TX}: transmitter output power	13 [dB]
D: path length	600 [m]
System losses due to:	
L_{TX}: transmitter lens	3.0 [dB]
L_d: beam divergence	23.8 [dB]
L_t: atmospheric turbulence	3.0 [dB]
L_s: aerosol scattering	1.3 [dB]
L_a: molecular absorption	0.3 [dB]
L_{RX}: receiver lens	3.0 [dB]
$L: = L_{TX} + L_d + L_t + L_s + L_a + L_{RX}$	34.4 [dB]
P_{RX}: receiver signal level	–21.4 [dB]
Receiver threshold at BER = 1.10^{-3}	–31 [dB]
Fade margin	9.6 [dB]

Table 1. The link budget shows that the loss due to beam divergence is very high compared to the others losses. This highlights the poor collimating quality of the lens: the more collimated the transmitted beam, the smaller the divergence is.

ture, relative humidity, barometric pressure) and the digital pseudo-random binary sequence. The AGC signal is simultaneously measured and recorded on a chart paper-recorder. The chart paper-recorder is used for quick visual control and to get instantaneous indications of the atmospheric effects on the received signal. Data are collected at a rate of 20 samples per second. The incoming digital pattern is analyzed by an error detector test set at a 1-s gating time. The data stored on the hard disc of the data acquisition computer are periodically transferred via ethernet onto a high-capacity magneto-optical disc. As it can be seen in Figure 1b, a second computer used for the assessment of the recorded data is connected to this magneto-optical disc.

Safety requirements for the use of laser heads under test

There are strict rules to observe when using a laser head. Because the lens of the human eye can focus the narrow laser beam to intense beams on the retina, there are inherent potential dangers in using a laser beam [2, 3]. The danger is especially critical when invisible light is concerned; therefore, direct viewing into the laser source must be strictly avoided. In cases of uncertainty, protective glasses must be worn. Furthermore, to protect persons who might not be aware of such a danger, the outdoor mounting of laser heads must be made so that the direct eye exposure within the field of the radiating source is impossible without using a special device. As a first warning against potential dangers of laser beams, commercial laser heads are categorized into various hazard classes according to their capability of causing damage to the eye. Every laser head bears a warning sign and explanatory label for the corresponding class. Furthermore, values of measured maximum permissible exposure (MPE), E_{max} [W/m^2], for various wavelengths from visible (0.4–0.7 μm) to invisible (0.7–1.4 μm) regions of the spectrum and the exposure time are listed [2]. Knowing the power density value of the laser beam that can cause irreversible damage to the eye, the minimum safety viewing distance D_{min} from the laser source under free-space conditions can be evaluated [2]:

$$D_{min}\,[m] = \frac{1}{\theta} \cdot \left(\sqrt{\frac{4 \cdot P_{TX}}{\pi \cdot E_{max}}} - d_{ill} \right)$$

where E_{max} [W/m^2] is the power density of the laser source, P_{TX} [W] the radiated power, d_{ill} [m] the diameter of the equivalent circular section of the laser beam at the receiver, and θ [rad] the beam divergence.

The laser head under test is categorized as Class 3B laser. Its MPE for λ = 0.78 μm is approximately E_{max} = 14.6 W/m^2 for a exposure time of 10 s. For $P_{TX} = 20 \cdot 10^{-3}$ W and $\theta = 1.2 \cdot 10^{-3}$ rad, the calculated minimum safety distance from the source is approximately D_{min} = 26.4 m. It should be noted that far away from the laser source the potential danger becomes very low because of both the divergence and scattering of the laser beam, which results in the reduction of the beam intensity when propagating through the atmosphere. More information about this topic, which is beyond the scope of this experiment, can be found in the references [2, 3], which are entirely devoted to it.

Results

In this section, statistical analyses of atmospheric effects on the received signal are carried out. Description of recorded effects and their correlation with atmospheric parameters are also presented. The period of data collection and analysis extends over a 16-month period. Prior to the field trial, climatic room measurements were carried out on the amount of beam deflection in function of temperature variations (–20 to +40 °C). Results showed negligible effects for a maximum of 1 km path length.

Statistical results

During the period of data collection, under various weather conditions (rainfall, snowfall, fog, haze, very warm sunshine, etc.), one realizes that the performance of the transmission system could be severely affected depending on the weather conditions. There were in particular several interruptions mainly due to dense fog (i.e. optical visibility ≤ path length) or snows storms, but no interruption due to failure of test equipments occurred. The system was operational during 89.4 % of the total data collection time.

Very poor availability of the link was recorded during periods of foggy weather (31 % of the period of time of operation), whereas the longer availability period (94.6 %) was recorded in spring.

Some representative measured specific attenuations relative to the free-space value for this path are given in Table 2. It shows that attenuations due to dense fog, snowfall and intense rainfall (> 2.5 mm/min) are very high compared to other atmospheric effects.

Distributions of fade depths

Figure 2 shows the monthly cumulative distributions of fade depth events. The fade depths are expressed relative to the received signal level (P_{AX} = – 22 dBm) under free-space propagation conditions. All atmospheric effects are included in these statistics. As it can be seen in Figure 2, the probabilities of exceeding of the fade margin of 9 dB (corresponding to the receiver threshold at BER [bit error tate] = 10^{-3}) are higher than 20 % every month. From Figure 2 it can be derived that a fade margin of 18 dB will result in a reduction of the percentage time the receiver threshold is exceeded, from 20 % to 0.001 %. An easy and straightforward way of obtaining such a reduction is to reduce the path length, for instance to 250 m.

Quality and availability

Availability and quality of the transmission performance are assessed according to the ITU-T Rec. G.821 [4, 5]. The periods of unavailable time of the link are expressed in terms of *non-available seconds* (NAS), and the system quality in terms of error performance parameter which are *errored seconds* (ES), and *severely errored seconds* (SES). The error measurements were made at the system bit rate, i.e. 2.048 Mbit/s; one second with one error corresponds to a BER = $4.9 \cdot 10^{-7}$.

Figure 3 shows the total number of ES, SES and NAS for the complete measurement period which is given on a monthly basis. The numbers of NAS are often larger than those of ES and SES. October represents the worst month for the NAS parameter. Differences between monthly results of 1993 and 1994 reflect the annual variability in seasons. In Figure 4 the frequency of occurrence of NAS events of a given duration are shown. Figure 4 highlights the fact that when the fading events occurred, they lasted more than 60 s. Table 3 shows results for worst-month recorded values. As it can be seen, the performance objectives for this link are not fulfilled.

Meterological conditions	Specific attentuation (dB/km)
Sunny clear weather (optical visibility > 5 km; $T_0 \approx 20$ °C, H ≈ 65 %, P ≈ 947 hPa)	5 to 13
Light fog (visibility ≥ path length)	5 to 17
Dense fog (visibility < path length)	>22
Wet snowfall	15 to 21
Rainfall (> 2.5 mm/min)	>15

Table 2. Measured atmospheric specific attenuations relative to the free-space value at 0.78 μm over the path length of 600 m. (T_0 is the air temperature, *H* the relative humidity, and *P* the barometric pressure.)

Error parameters	Worst months			Performance objectives for this link
	May 93	June 93	Oct. 93	
ES	–	$3.7 \cdot 10^{-1}$	–	$9.6 \cdot 10^{-4}$
SES	$3.4 \cdot 10^{-2}$	–	–	$9.6 \cdot 10^{-7}$
NAS	–	–	$4.7 \cdot 10^{-1}$	$1.2 \cdot 10^{-5}$

Table 3. Measured quality and unavailability statistics according to ITU-R G.821 and comparison with performance objectives of Telecom PTT.

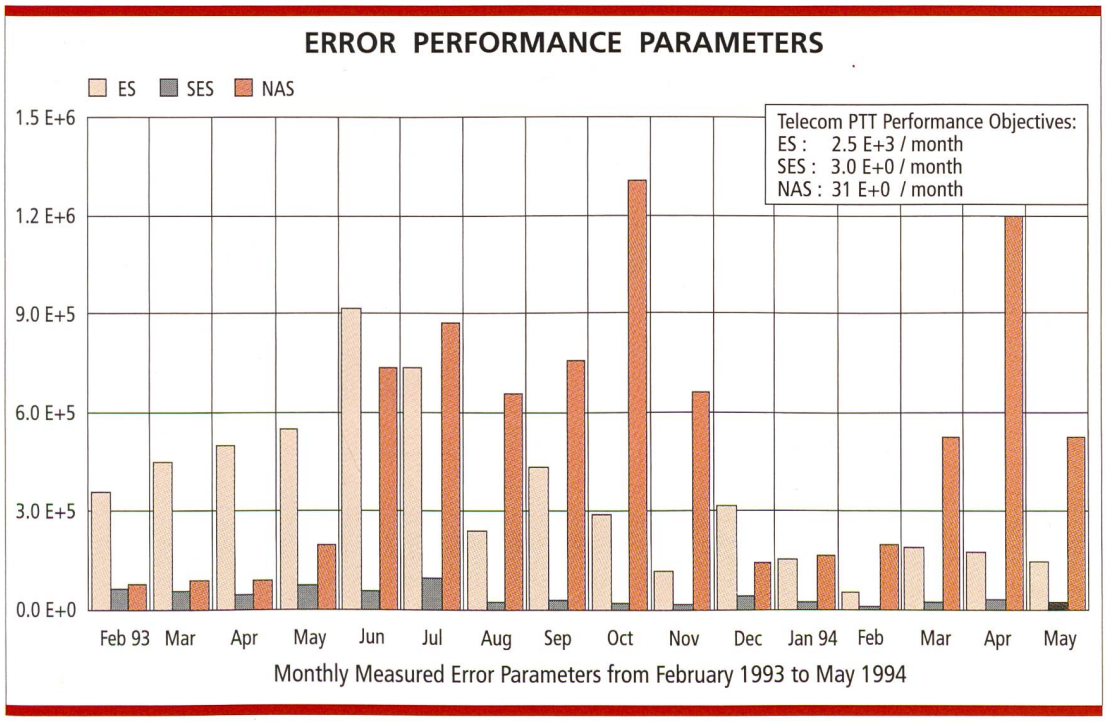

Fig. 3. Error performance parameters. Errored seconds (ES), severeley errored seconds (SES), nonavailable seconds (NAS).

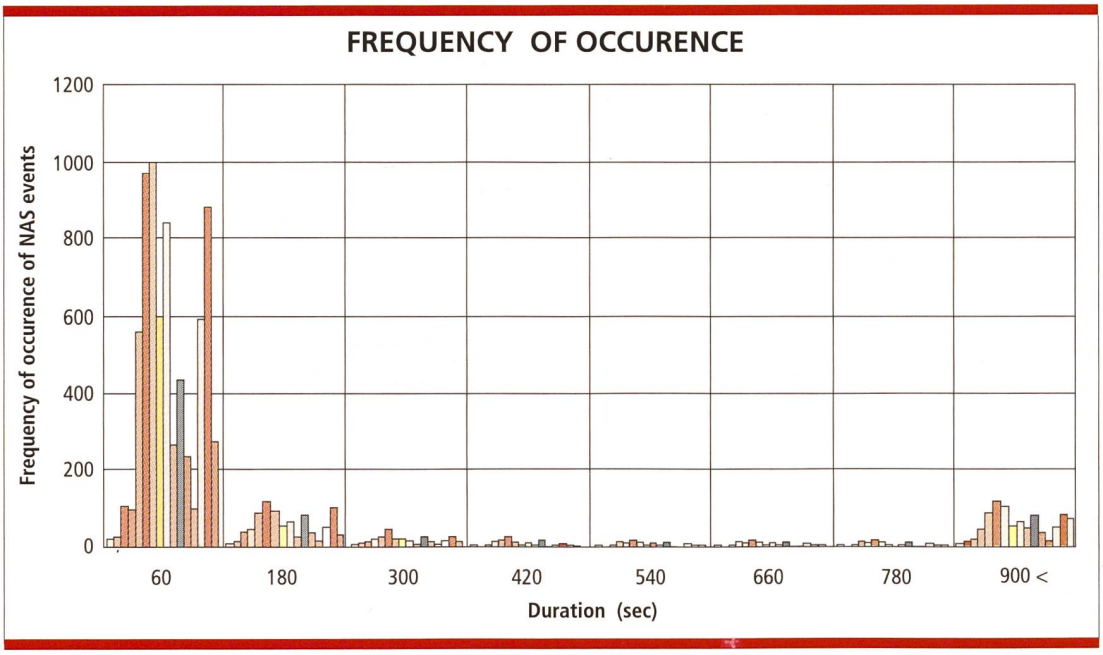

Fig. 4. Frequency of occurrence of NAS events of a given duration. Measured data from 1 February 1993 to 31 May 1994.

Atmospheric effects and their correlation with the meteorological parameters

In this section we will attempt to identify the dominant causes of the degradations of the received signal and their correlation with the meteorological conditions. It is important to keep in mind that all recorded effects are interrelated.

Effects of clear-air weather

In the absence of attenuation caused by identifiable phenomena such as fog, snowfall, and rainfall, under conditions of good visibility (sunny, clear-air weather), the atmospheric channel severely affects the signal level which exhibits strong fluctuations (scintillations) on a millisecond scale. The received signal level recorded during sunny warm days (Figures 5 to 7) shows large amplitude fluctuations with occurences of BER often higher than 10^{-4}.

The recorded effects are due to *atmospheric turbulence*. The upwards movement of heated dusty air due to both the heating of the earth's surface by the sun as well as to human activities (heating, traffic, pollutants) gives rise to atmospheric temperature fluctuations which in turn cause atmospheric turbulence. Atmospheric turbulence is a random process which causes beam spreading and even random changes in beam direction of propagation, which in turn lead to large fluctuations in the received signal level. Based on the measured values of the air temperature T_0 (°C), the relative humidity H (%), and the barometric pressure P (hPa), a reliable estimate of the atmospheric refractivity N (N-units) at the optical wavelengths can be obtained from [6]:

$$N = 77.6 \cdot [1+7.52 \cdot 10^{-3} \cdot \lambda^{-2}] \cdot \frac{P}{T}$$

and, the water vapour concentration ρ (g/m³) [7]:

$$\rho = 2.167 \cdot \frac{H}{T} \cdot 6.1121 \cdot \exp\left(\frac{17.502\, T_o}{(T_0+240.97)}\right)$$

where T is the absolute temperature (K) and λ is the wavelength (μm).

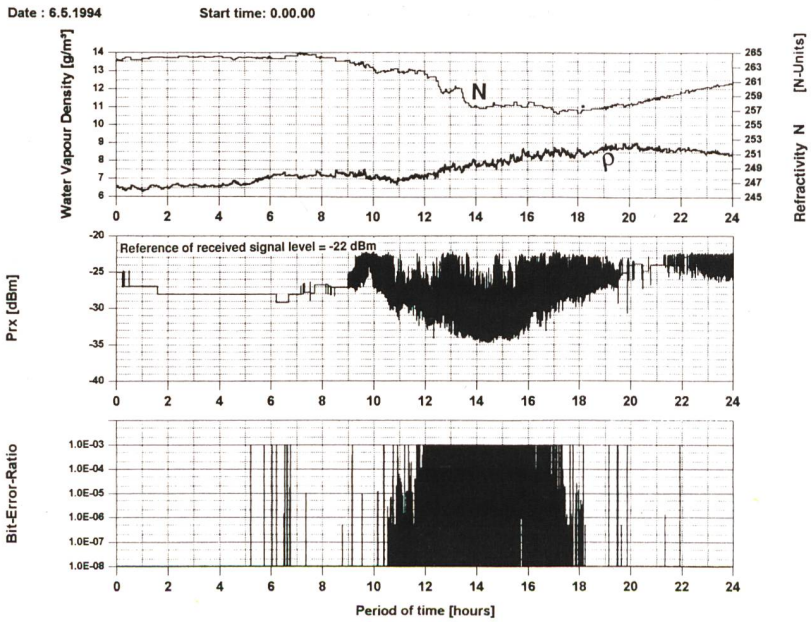

Simultaneous recordings of
- water vapour density in air ρ (g/m³) and atmospheric refractivity N (*N*-units),
- amplitude fluctuations of the received signal Prx (dBm) and
- bit error ratio

at the wavelength of 780 nm and a transmission rate of 2.048 Mbit/s on a 600-m path length
Observation period: 24 hours, starting at 00.00.00 on 6 May 1994

Fig. 5. Simultaneous recordings of water vapour density in air, atmospheric refractivity, amplitude fluctuations of the recieved signal, and bit error ratio on 6 May 1994.

From Figures 5 to 7, the simultaneous recordings of received signal level (P_{RX}), BER and related meteorological parameters show to what extent variations in refractivity N give rise to fluctuations in the received signal level and occurrences of bit errors. Occurrences of BER = 10^{-3} are due to wavefront distortions.

In Figures 5 and 6, during the period of time from 00.00 to 06.00, attenuation occurred in the received signal level. Since no variation in the water vapour concentration ρ was recorded during this period of time, this attenuation may be due to condensation effects on the receiver lens.

Effects of rainfall

Annual and worst month statistics on the percentage of time that a given rain rate is exceeded are presented in Figure 8. For comparison, the ITU-R rainrate distribution [8] for K zone (ITU-R repartition of rain climate regions on the globe) is also drawn in Figure 8; it is in agreement with the measured curve.

Figures 9 and 10 show simultaneous recordings of rainfall intensities, received signal level, and bit error rate. The impact of the rainfall on the transmission quality is obvious: the receiver threshold value is exceeded during periods of rainfall. Signal degradation result from scattering effects. We observed occurrences of sporadic bit errors due to small rain-drops. Simulation of the observed phenomena show that small drops of water of the same order of size as the outgoing laser beam can deflect the laser beam, giving rise to received signal attenuation and BER <10^{-3}, or can cause wavefront distortions without received signal attenuation, but with BER >10^{-3}. In order to reduce the impact of such scattering effects on the received signal, the diameter of the receiver collecting lens can be increased, or/and the diameter of the outgoing laser beam can be expanded prior to collimating.

Effects of foggy weather

Depending on its density, *fog reduces or obstructs the optical visibility between the transmitter and the receiver.* A typical measurement of the effects of fog on the received signal is shown in the paper-recorder chart in Figure 11a. This plot of a 5-h observation period shows very fast variations in the re-

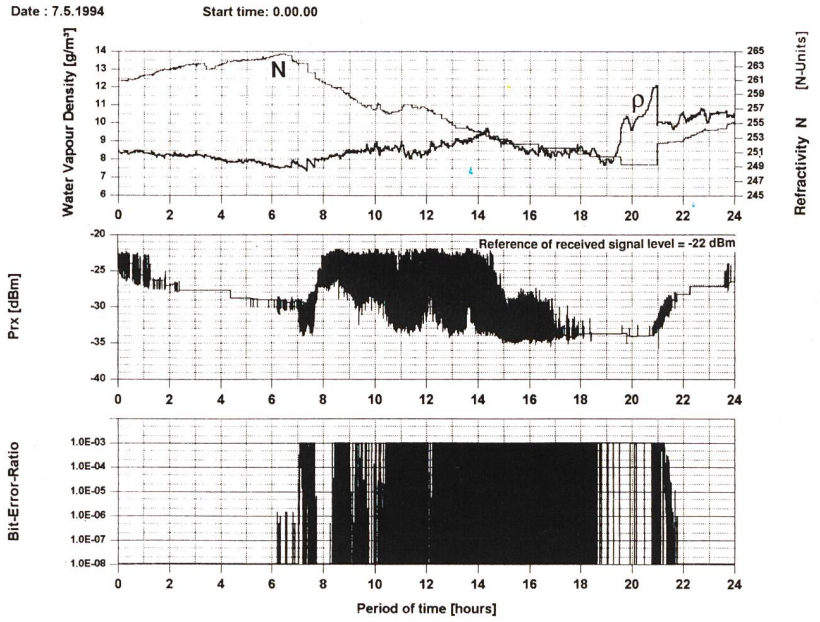

Simultaneous recordings of
– water vapour density in air ρ (g/m³) and atmospheric refractivity N (*N*-units),
– amplitude fluctuations of the received signal Prx (dBm) and
– bit error ratio
at the wavelength of 780 nm and a transmission rate of 2.048 Mbit/s on a 600-m path length
Observation period: 24 hours, starting at 00.00.00 on 7 May 1994

Fig. 6. Simultaneous recordings of water vapour density in air, atmospheric refractivity, amplitude fluctuations of the recieved signal, and bit error ratio on 7 May 1994.

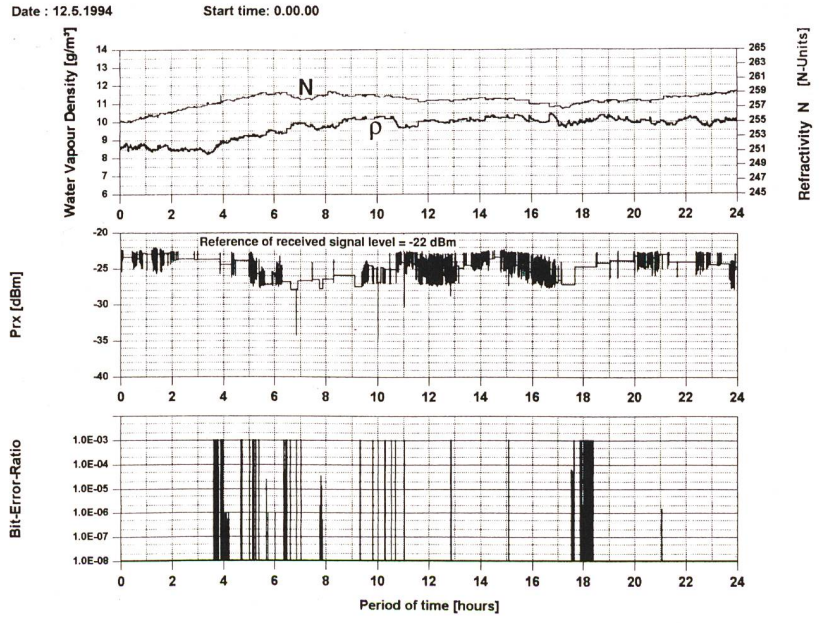

Simultaneous recordings of
– water vapour density in air ρ (g/m³) and atmospheric refractivity N (*N*-units),
– amplitude fluctuations of the received signal Prx (dBm) and
– bit error ratio
at the wavelength of 780 nm and a transmission rate of 2.048 Mbit/s on a 600-m path length
Observation period: 24 hours, starting at 00.00.00 on 12 May 1994

Fig. 7. Simultaneous recordings of water vapour density in air, atmospheric refractivity, amplitude fluctuations of the recieved signal, and bit error ratio on 12 May 1994.

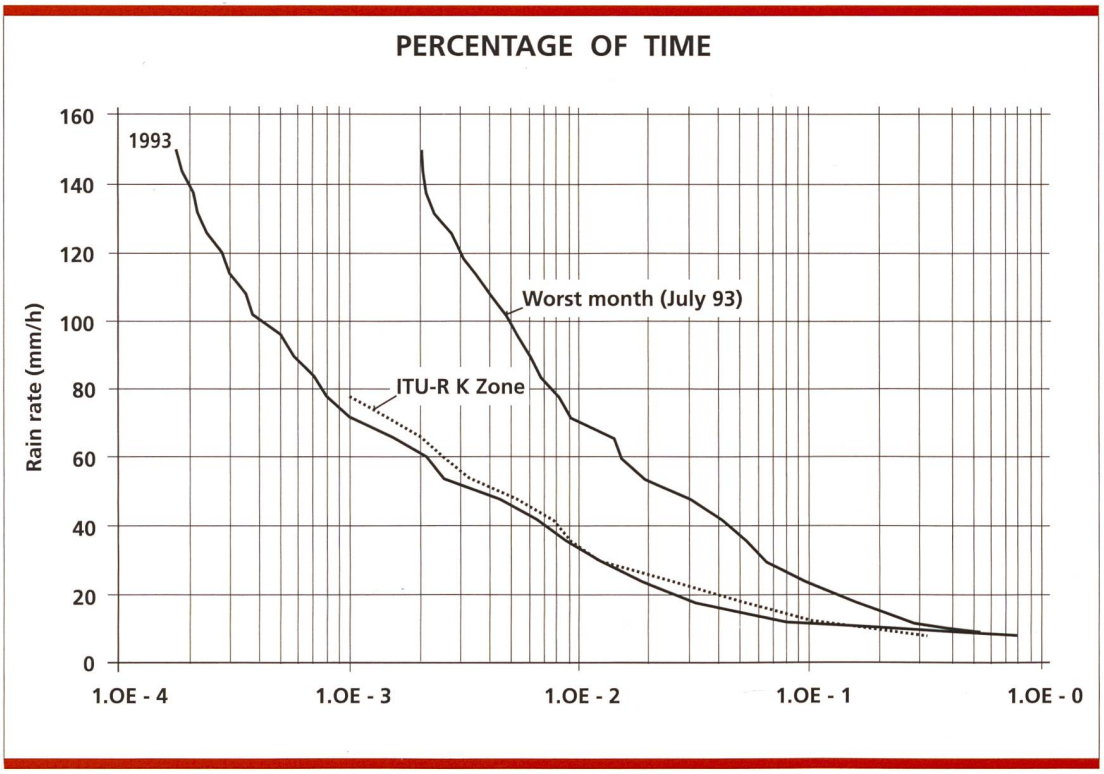

Fig. 8. Percentage of time the rain rate is exceeded.

ceived signal level on a time scale of a few seconds as well as a flat fade of about 6 dB. The flat fade value is time varying depending on the behaviour and the density of the fog. When the density of the fog is such that the receiver cannot 'see' the transmitter, it results in an outage (period of time with BER $>10^{-3}$). Depending also on wind conditions, long periods of dense fog may periodically be alternated with very short periods of light fog.

Effects of snowfall

Figure 11b shows typical effects of snowfall on the received signal for an observation period of 5 h. The recorded snowfall lasted throughout that day. The rain-equivalent snowfall rates were between 0.1 mm/h and 1.3 mm/h. *Depending on the snowfall rate and the size of the snow flakes, snowfall also reduces or obstructs the visibility between the transmitter and the receiver.* Due to the behaviour of the received signal it became obvious (Figure 11b) that long periods of snowfall were from time to time alternated with short periods of slight snowfall during which the receiver was able to 'see' the transmitter. The impact of snowfall on the transmission quality is evident from the statistics of BER shown in Figure 11 for an observation period of 24 h.

Concluding remarks

Advantages of point-to-point communication links with an atmospheric laser system were mentioned in the introduction; however, based on the results obtained so far with the 0.78-µm laser-based system over 600 m path length, the following limitations on the system performance have also been observed:

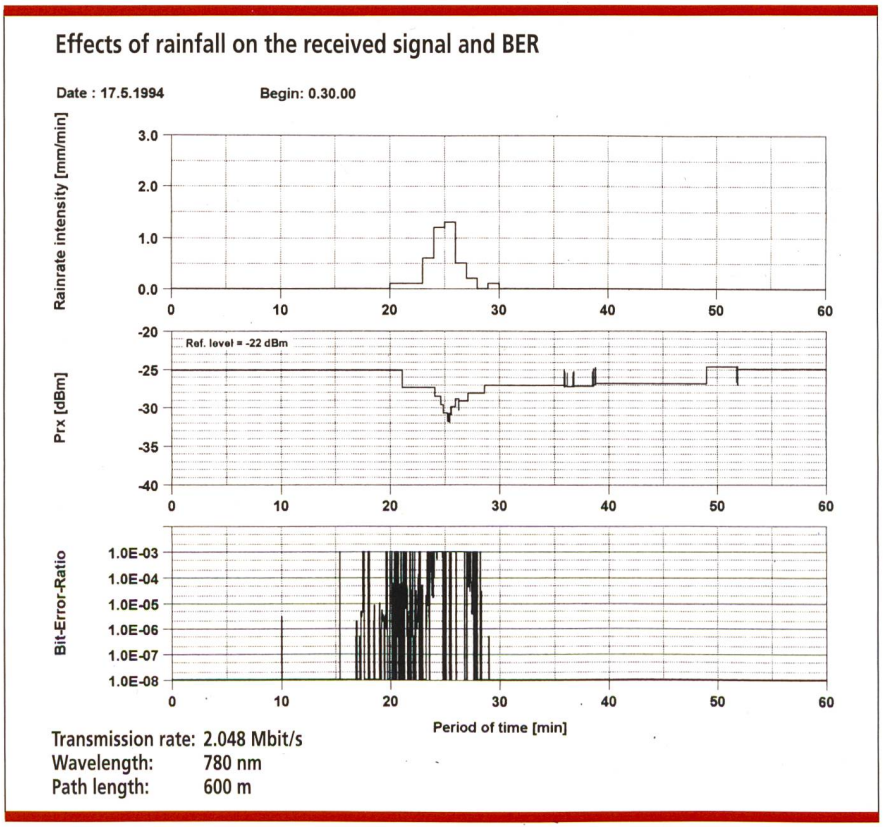

Fig. 9. Simultaneous recordings of rain rate, recieved signal, and bit error ratio on 17 May 1994.

List of symbols

P_{TX} [dBm]	radiated transmitter power
D [m]	length of the optical path
λ [m] = c/f	wavelength
$c \approx 3 \cdot 10^8$ m/s	speed of light
f [Hz]	frequency
θ [mrad] = $(d_{ill} - d_{TX})/D$	beam divergence
A_{RX} [m^2] = $\pi \cdot (d_{RX}/2)^2$	surface area of the receiver collecting lens
A_{TX} [m^2] = $\pi \cdot (d_{TX}/2)^2$	surface area of the transmitter collimating lens
A_{ill} [m^2] = $\pi \cdot (d_{ill}/2)^2$	equivalent circular section of the beam at the receiver
P_{RX} [dBm]	receiver power level
$P_{RXseuil} = -31$ [dBm]	receiver power threshold at BER = $1 \cdot 10^{-3}$
L [dB]	system losses budget
L_{TX} [dB]	transmitter lens attenuation
L_{RX} [dB]	receiver lens attenuation
L_t [dB]	loss due to turbulence
$L_s = \exp(-\alpha s\,[\lambda] \cdot D\,[km])$*	loss due to scattering
$\alpha s = \frac{3.91}{V\,[km]} \cdot \frac{\lambda\,[\mu m]^{-\delta}}{0.55}$	scattering coefficient
$V = 5.5$ km $\delta = 0.585V^{0.333} \approx 1.03$	average optical visibility
$L_a = \exp(-\alpha a\,[\lambda] \cdot \sqrt{D\,[m]})$*	loss due to molecular absorption
$\alpha a = 0.0305 \cdot \sqrt{\frac{w}{D\,[m]}}$	absorption coefficient
$w = D \cdot \rho \cdot 10^{-3}$ [mm]	equivalent water content along the optical
$L_d = \frac{\Omega_{RX}}{\Omega_{ill}}$	attenuation due to beam divergence
$\Omega_{RX} = \frac{A_{RX}}{D^2}$ [sr]	solid angle subtended by A_{RX}
$\Omega_{ill} = \frac{A_{ill}}{D^2}$ [sr]	solid angle subtended by A_{ill}

* Weichel H.: *Laser Beam Propagation in the Atmosphere,* SPIE's Tutorial Texts in optical engineering, Vol. TT3, 1990.

References

[1] ITU-R Rep 883-2: Attenuation of visible and infrared radiation. Annex to Vol. 5, 1990.

[2] IEC 825: Radiation safety of laser products, equipment classification, requirements and user's guide. IEC Publication, 1984.

[3] Winburn D. C.: Practical laser safety. Occupational safety and health/11, Marcel Dekker, Inc., 1985.

[4] ITU-T Rec. G.821: Error performance of an international digital connection operating at a bit rate below the primary rate and forming part of an integrated services digital network. May 1996.

[5] ITU-R Rec. F 697-2: Error performance and availability objectives for local-grade portion at each end of an ISDN connection at a bit rate below the primary rate utilizing digital radio-relay systems. 1996 F Series Vol., part 1.

[6] Clifford S. F.: The classical theory of wave propagation in a turbulent medium. Topics in Applied Physics, Vol. 25, p. 9., 1978. Springer-Verlag, New York.

[7] ITU-R Rec. P 453-5:The Radio Refractive Index: its formula and refractivity data. Radio propagation, 1996 P Series Vol.

[8] ITU Rec. P 837-1: Characteristics of precipitation for propagation modelling. 1994 PN Series Vol., Propagation in nonionized media.

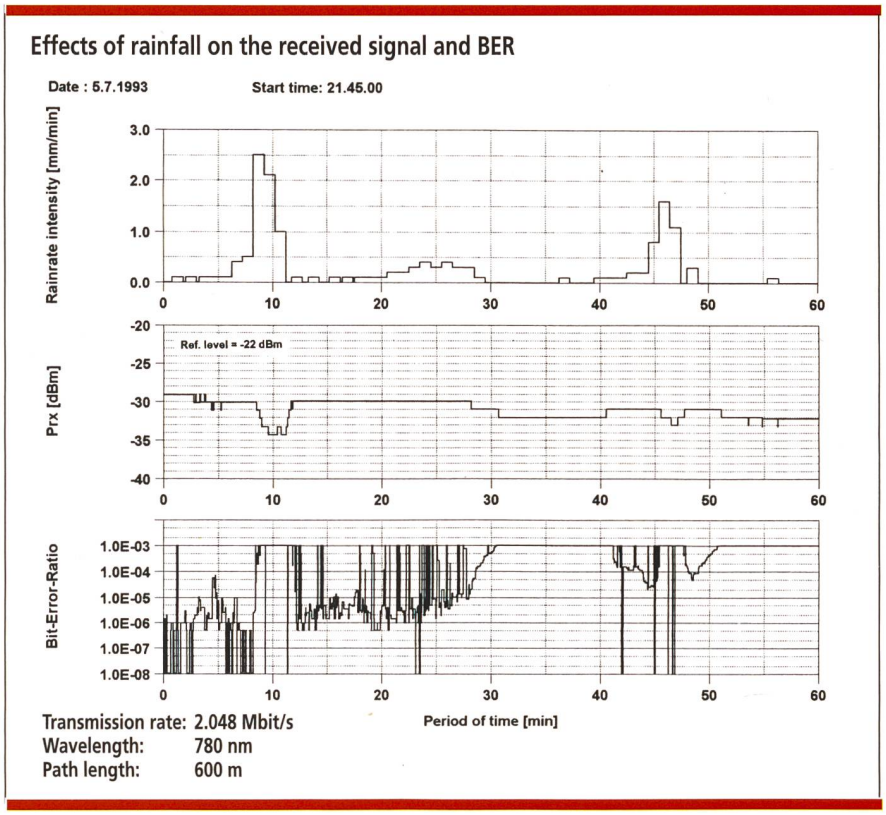

Fig. 10. Simultaneous recordings of rain rate, recieved signal, and bit error ratio on 5 July 1994.

- Dense fog, heavy snowfall and atmospheric turbulence strongly reduce the availability and the quality of the system.
- Due to its small fade margin (9 dB) the receiver threshold ($P_{RX} = -31$ dBm at BER = 10^{-3}) is almost always exceeded for long periods of time.
- The wavelength ($\lambda = 0.78$ μm) under test is not appropriate for terrestrial long distance (more than 500 m) communication through a turbulent atmosphere or important aerosol concentration. Longer wavelengths ($\lambda > 10$ μm) should be considered for future investigations.

Furthermore, in order to reduce the beam intensity losses due to scattering, the diameter of the outgoing laser beam should be expanded prior to collimating, and the diameter of the re-

Numerical evaluations for standard atmosphere

$H = 60$ %; $T_0 = 15$ °C; $P = 1013$ hPa;
$\rho = 7.5$ g/m^3
P_{RX} [dBm] = P_{TX} [dBm] – L [dB]
≈ 22 [dBm]
$L = L_{TX} + L_d + L_t + L_s + L_a + L_{RX}$
≈ 34.4 [dB]
$P_{TX} = 13$ [dBm]
$L_{TX} = 3$ [dBm]
$L_d = 23.8$ [dB]
$L_t = 3$ [dB]
$L_s = 1.3$ [dB]
$L_a = 0.3$ [dB]
$L_{RX} = 3$ [dB]
$D = 600$ [m]
$\lambda = 0.78$ [μm]
$\theta = 1.2 \cdot 10^{-3}$ [rad]
$A_{RX} = 1.7 \cdot 10^{-3}$ [m^2]
$A_{TX} = 78.5 \cdot 10^{-6}$ [m^2]
$A_{ill} = 0.41$ [m^2]
$P_{RX} = -22$ [dBm]
$\Omega_{RX} = 4.72 \cdot 10^{-9}$ [sr]
$\Omega_{ill} = 4.52 \cdot 10^{-6}$/[sr]
$\alpha a = 2.64 \cdot 10^{-3}$
$\alpha s = 0.5$

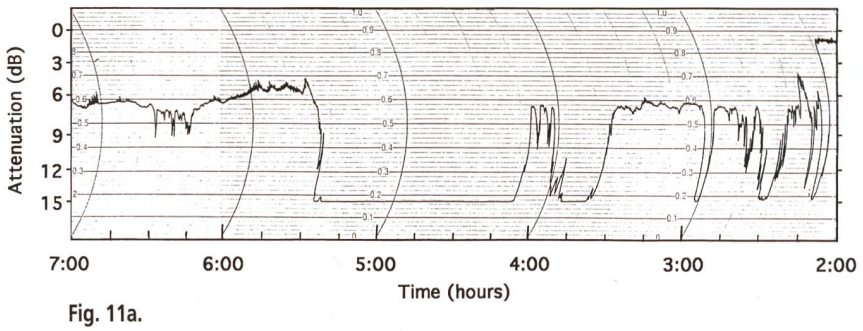

Fig. 11a.

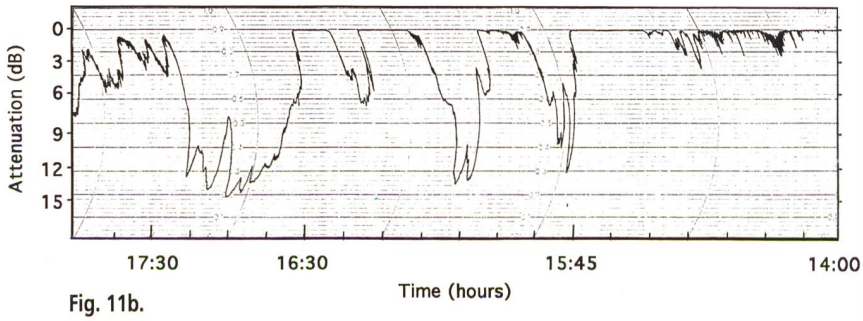

Fig. 11b.

Fig. 11. Effects of dense fog on 16 February 1993 (a) and wet snowfall on 23 February 1993 (b) on the recieved signal.

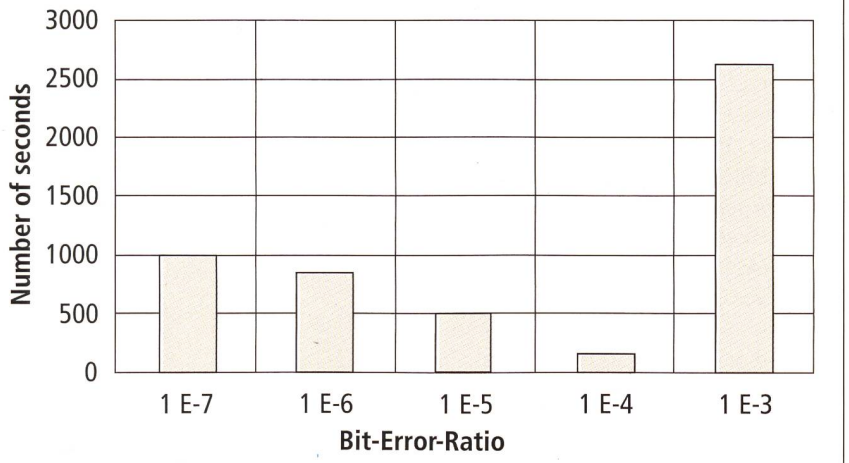

Fig. 11c.

ceiver collecting lens should be increased (limit is given by the cross-section of the radiated beam at the receiver plan), so as to intercept as much power as possible.

– Nevertheless, the system under test can be used for a short path length transmission, e.g. 250 m. Such a path-length shortening will result in an increase of the fade margin, which will satisfy the performance objectives of Telecom PTT.

ZUSAMMENFASSUNG

Lasergestützte Direktverbindung durch die Atmosphäre

In einem Feldversuch wurde der Einfluss des Wetters auf die Übertragungsqualität einer lasergestützten Direktverbindung durch die Atmosphäre ermittelt. Die Beurteilung des über ein Jahr lang betriebenen Versuchsaufbaus erfolgte gemäss ITU-T Rec. G.821. Dabei zeigte sich, dass dichter Nebel längere Unterbrechungen der Verbindung zur Folge hat und Schneefall die Übertragungsqualität stark vermindert. Die Richtlinien der Telecom PTT erfüllt das untersuchte System erst bei sehr kurzen Übertragungsstrecken.

Acknowledgement

I would like to express my thanks to all my colleagues of FE 433, in particular to D. Vergères for his suggestions, M. Ebner and M. Matter for their technical support. 8.4

Loémbé André is an engineer in the group FE 433 (satellite communications technology and microwave systems). He graduated in electrical engineering from the Swiss Institute of Technology (EPF Lausanne) and received his doctor's degree from the French Ecole Nationale Supérieure des Telecommunications (ENST, Paris). In 1987, he joined the Swiss Telecom PTT research center, as engineer, where he has since worked on various line-of-sight digital communications systems and on atmosphere effects on the radiowave propagation. His current activities include experimental research on digital transmission performance of microwave, millimetre wave and laser-based communication systems. He has been active in COST Project 235 as expert and also participated in the works of the ITU-R Study Group 3 (WG 3J and 3M).